Biochimica et Biophysica Acta 1837 (2014) 643–655

Contents lists available at ScienceDirect

Biochimica et Biophysica Acta

journal homepage: www.elsevier.com/locate/bbabio

Review

Channelrhodopsins: A bioinformatics perspective ☆

Coral del Val [a,*,1], José Royuela-Flor [b], Stefan Milenkovic [b], Ana-Nicoleta Bondar [b,*,2]

[a] Department of Computer Science and Artificial Intelligence, University of Granada, 18071 Granada, Spain
[b] Theoretical Molecular Biophysics, Department of Physics, Freie Universitaet Berlin, 14195 Berlin, Germany

ARTICLE INFO

Article history:
Received 1 July 2013
Received in revised form 7 November 2013
Accepted 9 November 2013
Available online 16 November 2013

Keywords:
Channelrhodopsin
Bioinformatics
Membrane protein
Protein structure and dynamics

ABSTRACT

Channelrhodopsins are microbial-type rhodopsins that function as light-gated cation channels. Understanding how the detailed architecture of the protein governs its dynamics and specificity for ions is important, because it has the potential to assist in designing site-directed channelrhodopsin mutants for specific neurobiology applications. Here we use bioinformatics methods to derive accurate alignments of channelrhodopsin sequences, assess the sequence conservation patterns and find conserved motifs in channelrhodopsins, and use homology modeling to construct three-dimensional structural models of channelrhodopsins. The analyses reveal that helices C and D of channelrhodopsins contain Cys, Ser, and Thr groups that can engage in both intra- and inter-helical hydrogen bonds. We propose that these polar groups participate in inter-helical hydrogen-bonding clusters important for the protein conformational dynamics and for the local water interactions. This article is part of a Special Issue entitled: Retinal Proteins — You can teach an old dog new tricks.

1. Introduction

The microbial-type channelrhodopsins (ChRs) are light-gated cation channels that can be used as powerful optogenetic tools [1–4]. These proteins contain a transmembrane rhodopsin domain, where cation transport occurs [5–7]. The retinal chromophore is covalently attached to a conserved Lys on transmembrane helix G. Experiments on *Chlamydomonas reinhardtii* ChR-2 indicate that in the resting state of the protein, the retinal configuration is a mixture of all-trans, 13-cis, and 9-cis isomers, the all-trans isomer being predominant [8]. Upon absorption of light the all-trans retinal isomerizes to 13-cis, triggering a reaction cycle during which the protein passes through four main intermediate states, P1–P4, distinguished by their spectral fingerprints [9,10], protein conformation, or hydrogen bonding and protonation state of specific carboxylate groups [10–12].

Our understanding of channelrhodopsins benefits from the detailed knowledge of the structures and mechanisms of other microbial rhodopsins. But the mechanism of action of channelrhodopsins might be very different: Albeit the recent structure of a channelrhodopsin chimera structure [13] indicates that the overall fold of channelrhodopsins is similar to that of, e.g., the bacteriorhodopsin proton pump (BR), the sequence of the rhodopsin domain of ChR-2 has less than 20% identity with that of BR [6]. This is somewhat less than the ~30% identity for the sequences of BR and the halorhodopsin chloride pump, or for BR and sensory rhodopsin II.

Comparisons of the BR and ChR sequences, structures, and mechanisms of action are important for our general understanding of how pumps and channels may work. Indeed, it was suggested that channelrhodopsins may have evolved from pump microbial rhodopsins 'by loss or uncoupling of a gate' [14], though details of the relationship between BR and channelrhodopsins can depend on the channelrhodopsin variant [15,16]. It is thus intriguing that in special conditions ChR-2 might act as a pump [17]. Knowing which of the differences in sequence and molecular interactions of BR vs. channelrhodopsins are essential for the channel functionality is important, because it may assist in selecting mutations to fine-tune the selectivity of channelrhodopsins for specific cations, or its conformational dynamics.

Experiments on various channelrhodopsins led to valuable information regarding specific amino-acid residues and interactions important for various aspects of channelrhodopsin function (see, e.g., refs. [2,3,10,11,13,18–25]), and the identity of carboxylate groups that undergo protonation changes (e.g., refs. [11,12]). Understanding the molecular origin of the effects of mutations investigated with experiments is made difficult by the scarcity of the structural information on channelrhodopsins. To date, there is only a low-resolution (6 Å) cryo-electron microscopy structure of the *C. reinhardtii* ChR-2 C128T mutant [26] and an X-ray crystallography structure (2.3 Å resolution) of a *C. reinhardtii* ChR-1/ChR-2 chimera protein in which helices A-D are from ChR-1, and helices F-G from ChR-2 [13]. Prior to the release of the chimera crystal structure, several homology models of channelrhodopsins have been derived using as templates crystal structures of other microbial rhodopsins — see, for example, refs. [11,24,27]. Though the accuracy of these homology models is somewhat limited by the low sequence

☆ This article is part of a Special Issue entitled: Retinal Proteins — You can teach an old dog new tricks.

* Corresponding authors.
E-mail addresses: c.delval@decsai.ugr.es (C. del Val), nbondar@zedat.fu-berlin.de (A.-N. Bondar).
[1] Tel.: +34 958240468 (C. del Val).
[2] Tel.: +49 30 838 53583 (A.-N. Bondar).

0005-2728/$ – see front matter © 2013 Elsevier B.V. All rights reserved.
http://dx.doi.org/10.1016/j.bbabio.2013.11.005

identity between channelrhodopsins and the microbial rhodopsins used as a template, they proved useful for the interpretation of experimental results.

Here we use advanced bioinformatics tools to explore conservation patterns of channelrhodopsins, derive homology models of selected channelrhodopsin variants, and discuss the implications of sequences and structures for protein dynamics and function.

2. Sequence alignments of channelrhodopsins

Alignments of channelrhodopsin sequences provide valuable information for understanding aspects pertaining to the sequence/function relationship in channelrhodopsins and comparing channelrhodopsins with other microbial rhodopsins (e.g., refs. [2,13,27]); sequence alignments are also used for deriving homology models of channelrhodopsins (e.g., refs. [11,24,27]). The relatively low sequence identity between channelrhodopsins and other microbial rhodopsins and the insertion/deletions in the channelrhodopsin sequences can make difficult the derivation of accurate sequence alignments.

To align protein sequences, several algorithms with different heuristics could be used — for example, ClustalW [28], MAFFT [29], MUSCLE [30], T-Coffee [31], ClustalW being widely used. Although most of these algorithms use a progressive alignment [32], they differ in the pairwise scoring scheme: ClustalW [28] and MUSCLE [30] use a matrix-scoring approach to assess the cost of aligning two symbols, whereas T-Coffee incorporates more information in a consistency approach that is more accurate [33]. The pairwise scoring scheme leads to greater differences in the resulting alignments when the sequences do not share a homology higher than >40%, or when there are long insertions or deletions. Both the low sequence homology and the insertions/deletions require special attention when aligning sequences of channelrhodopsins with those of other microbial rhodopsins.

We chose T-coffee because it allows as input the combination of heterogeneous sources (e.g. sequence-alignment programs, structure alignments, threading, manual alignment, motifs and specific constraints). We used the T-Coffee strategy together with a template-based alignment using known PDB structures as a guidance available with the –pdb option of T-Coffee [31,34]. The initial alignment was performed using the T-coffee multiple sequence alignment package [31]. We combined sequence information with protein structural information to create a template-guided alignment by using the crystal structures of BR (PDB ID: 1QHJ, ref. [35]) and the ChR-1/ChR-2 chimera (PDB ID 3UG9, ref. [13]) from the Protein Data Bank [36]. The alignments obtained with T-coffee were then manually inspected and curated. The sequences used for channelrhodopsins and their data base entry codes are given in Fig. 1.

3. Motif searches, clustering, and alignment

Helix B of most channelrhodopsins studied here contains five Glu groups in the motif EExxxxxxExxxxxxExxxE, where by *x* we denote any amino acid. The presence of five Glu groups within a transmembrane helix is intriguing, because the membrane insertion of model helices with negatively-charged groups is energetically unfavorable [37]. To find out if other channel proteins may have the same motif, we performed a systematic search using the EMBOSS program fuzzpro [38], which allows searching for a specific pattern in a file of protein sequences. We performed several database searches for the Glu motif, one against the NCBI nr database, which is a non-redundant protein sequence database with entries from GenPept, Swissprot, PIR, PDB, and the NCBI (last 2012 release). Further searches were performed against the PDB (ref. [36], version June 2013) and the database of transmembrane proteins (PDB_TM, ref. [39]; version June 2013). The results obtained with fuzzpro for each of the databases were analyzed separately. To filter the information about the Glu motif signatures, we performed clustering using cd-hit (http://weizhong-lab.ucsd.edu/cd-hit/) [40]. The NCBI annotations of the proteins were added to the resulting clusters in order to compare functional annotations within a cluster and between the different clusters. Hypothetical proteins were neither further annotated nor used.

We examined the clusters to find out if they contain sodium, calcium, or potassium channels. The motifs belonging to the clusters of such channels were then independently aligned using the T-coffee multiple sequence alignment package [31]. Each of the alignments obtained with T-coffee for each set was manually inspected and curated by attending to relevant functional positions. The multiple sequence alignments were graphically represented with a sequence logo using the webser WebLogo (http://weblogo.berkeley.edu/examples.html). The sequence logo consists of stacks of letters. Each letter gives the amino acid residue, the height of the letter being an indication of its relative frequency of conservation. The overall height of a stack of letters indicates the sequence conservation measured in bits. In the cases where the alignment contained only few sequences we used the small sample correction of WebLogo [41].

The search against the NCBI nr pep database identified 11,940 sequences that presented at least one hit for the motif EExxxxxx ExxxxxxExxxE. 23.6% (2815) of these sequences were annotated as hypothetical or conserved hypothetical proteins without known function, and were discarded from further analysis.

4. Homology models of channelrhodopsins

A homology model of a query (target) protein can be obtained by first aligning the query sequence to that of a template protein whose crystal structure is known, and then using special algorithms to derive coordinates for the atoms of the target protein. More than one sequence and protein structures can be used as templates, the usage of multiple alignments being particularly important when the sequence identity between the target and the template(s) is low [42]. Proper alignment of the sequences of the target and template(s) is critical for the reliability of the homology model: for sequence identities of less than 30%, misalignments are a significant source of errors [42], i.e., a low similarity between the target and the template sequence can interfere with the accuracy of the alignment and of the homology model [42,43].

Numerous programs exist for deriving homology models of proteins — see, for example, Modeller [42,44], Medeller [45], Phyre [46], and the summary of web servers for homology modeling listed in ref. [46]. A critical discussion of the protocols used for the various homology-modeling algorithms is beyond the scope of this article.

To derive the homology models of channelrhodopsins we used the one-to-one threading option of the web-based program Phyre2 [46]. It was noted that the protocol used by Phyre allows the derivation of core homology model structures that are within 2–4 Å of the native structure even when the sequence identity between the target and the template is 15–20% [46].

As template for homology modeling we used either the ChR-1/ChR-2 chimera structure [13] or the BR structure [35]. For each channelrhodopsin, the query sequence used as input in Phyre2 was that of the rhodopsin domain obtained through the sequence alignments discussed in Section 2 above (for the full sequence alignments, see the Supplementary Information).

The high sequence identity between channelrhodopsins and ChR-1/ChR-2 (41% for *Mesostigma viride* ChR-1, 85% for *C. reinhardtii* ChR-1) as compared to the very low sequence identity (<20%) between channelrhodopsins and BR (Table 2) argue strongly for using the chimera structure as template for homology modeling. To illustrate the limitations of homology models of channelrhodopsin derived using templates with low sequence identity, we discuss briefly tests performed using BR [35] as a template.

Models of *C. reinhardtii* ChR-2 or of the ChR-1/ChR-2 chimera derived using BR as a template (Fig. 5A and B) have a core structure similar to that of the ChR-1/ChR-2 chimera (Fig. 3B) and the ChR-2

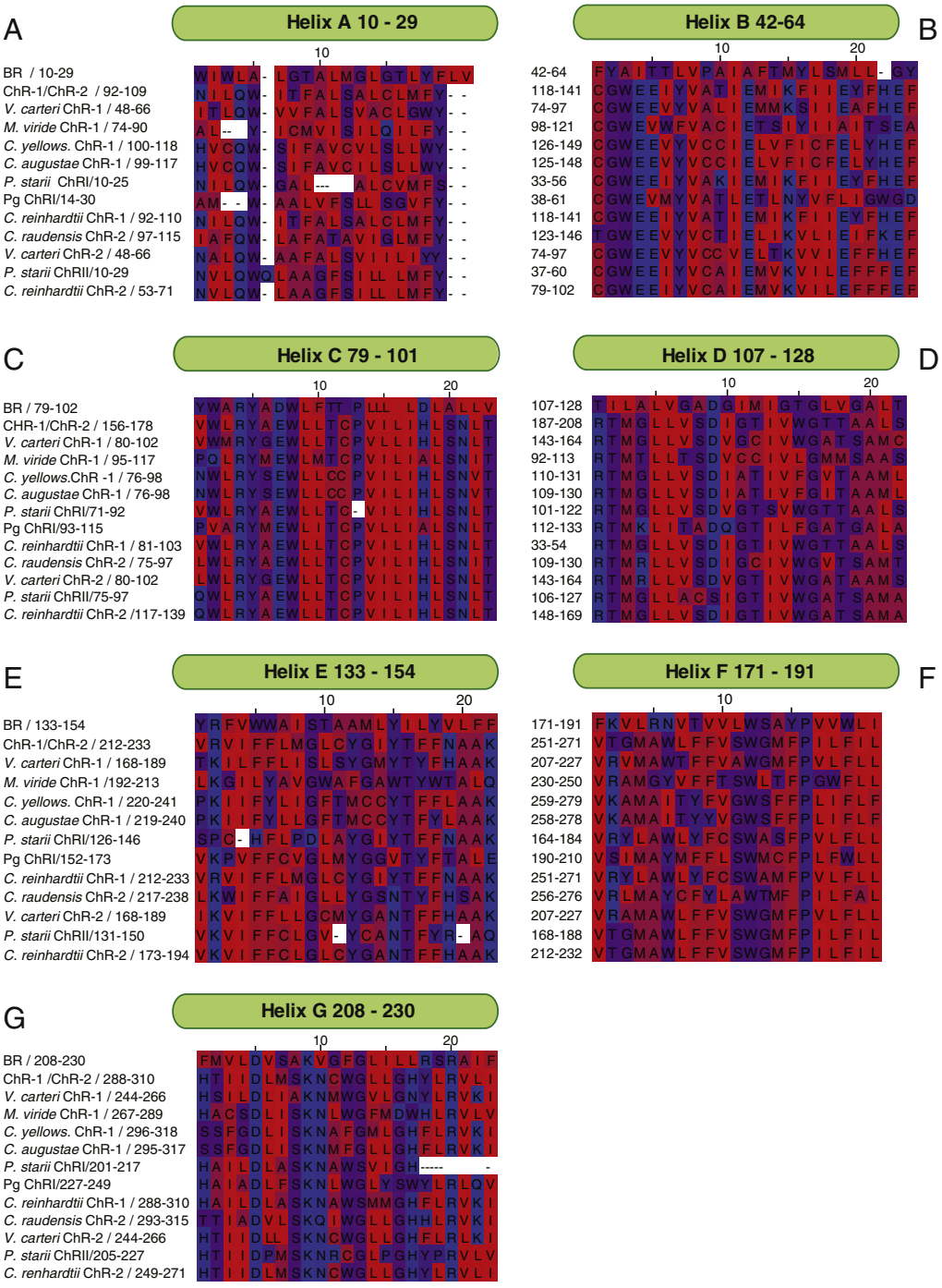

Fig. 1. Sequence alignments of channelrhodopsins. The sequence alignments are given for each of the seven helices (A–G) of bacteriorhodopsin (BR). The color scheme used is that of Kyte and Doolittle [104]. In this scheme, the amino acid residues are colored from red (most hydrophobic) to blue (most hydrophilic). The helical regions of BR were checked with the translocon analysis of MPeX [49]. The sequences used for BR and the ChR1/ChR-2 chimera are those of the protein structures from refs. [35] and [13], respectively. The UniProt entries for the other sequences are as follows: *Volvox carteri* ChR-1 — B4Y103; *M. viride* ChR-1 — F8UVI5; *Chlamydomonas yellowstonensis* ChR-1 — G8HK98; *Chloromonas augustae* ChR-1 — G8HKA1; *C. reinhardtii* ChR-1 — Q93WP2; *Chlamydomonas raudensis* ChR-2 — G8HK99; *V. carteri* ChR-2 — B4Y105; *C. reinhardtii* ChR-2 — Q8RUT8. The NCBI GenBank accession codes for *Pleodorina starii* ChR-1 and ChR-2 are AEY68812 and AEY68813, respectively. Pg ChR1 is the partial synthetic construct found under the GenBank code AEY68835.1 [2]. The complete sequence alignment is given in the Supplementary Information.

model derived using ChR-1/ChR-2 as a template (Fig. 3F). However, in the BR-based homology model of ChR-2 some polar and charged groups of helix B have an energetically unfavorable orientation whereby they face the hydrophobic membrane core (Fig. 5A). A similar observation of some of the helix B carboxylates of helix B pointing towards the exterior of the protein was made in the homology modeling work from ref. [24]. When subjecting the sequence of the rhodopsin domain of ChR-1/ChR-2 to homology modeling based on BR, the Glu groups of helix B have more reasonable orientations (Fig. 5B), but the overall orientation of the transmembrane helices appears somewhat closer to that of the BR template than of the ChR-1/ChR-2 crystal structure (Fig. 5C and

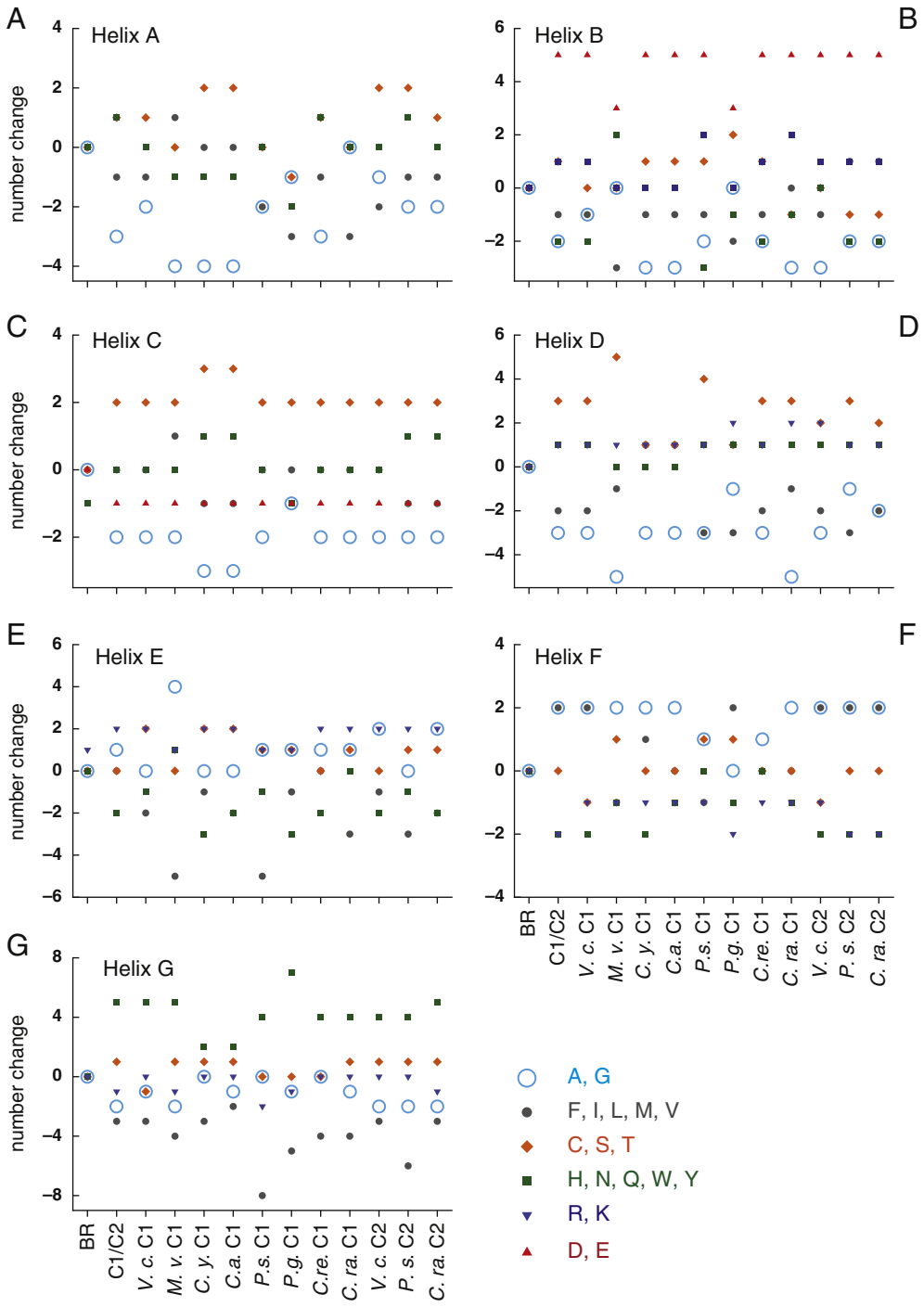

Fig. 2. Selected changes in amino acid sequence of channelrhodopsins relative to bacteriorhodopsin. The changes in amino acids were calculated for each of the helices A–G (panels A–G) based on the sequence alignments presented in Fig. 1. For clarity, we do not show changes in the composition of Pro groups. Pro groups are present in helices B, C, E and G (see Fig. 1).

D), indicating that specific interhelical interactions are not well reproduced.

The two BR-based homology models discussed above could be improved, for example, by manually editing the Phyre2 sequence alignment of the query and target sequences, and by subjecting the protein to structural optimization via molecular dynamics simulations. A protocol for homology modeling of channelrhodopsin is detailed, for example, in ref. [27]. But the accuracy of such a homology model in describing native intra-molecular interactions of channelrhodopsin would remain difficult to assess, and details of the model may depend on the stretch of the sequence of the channelrhodopsin target and on the protocol used to perform the sequence alignment, homology modeling, and structure optimizations. For the remaining of the manuscript we use in our discussion only those homology models derived based on the ChR-1/ChR-2 chimera structure from ref. [13] (Figs. 3 and 4), and for all sequence alignments we consider those derived using T-coffee [31].

5. The charged and polar groups of the transmembrane helices

To dissect patterns of conservation of the amino acids of channelrhodopsins, we use the sequence alignments of the transmembrane helical regions (Fig. 1, Table 1) and homology models of selected channelrhodopsins (Figs. 3–4, Table 2).

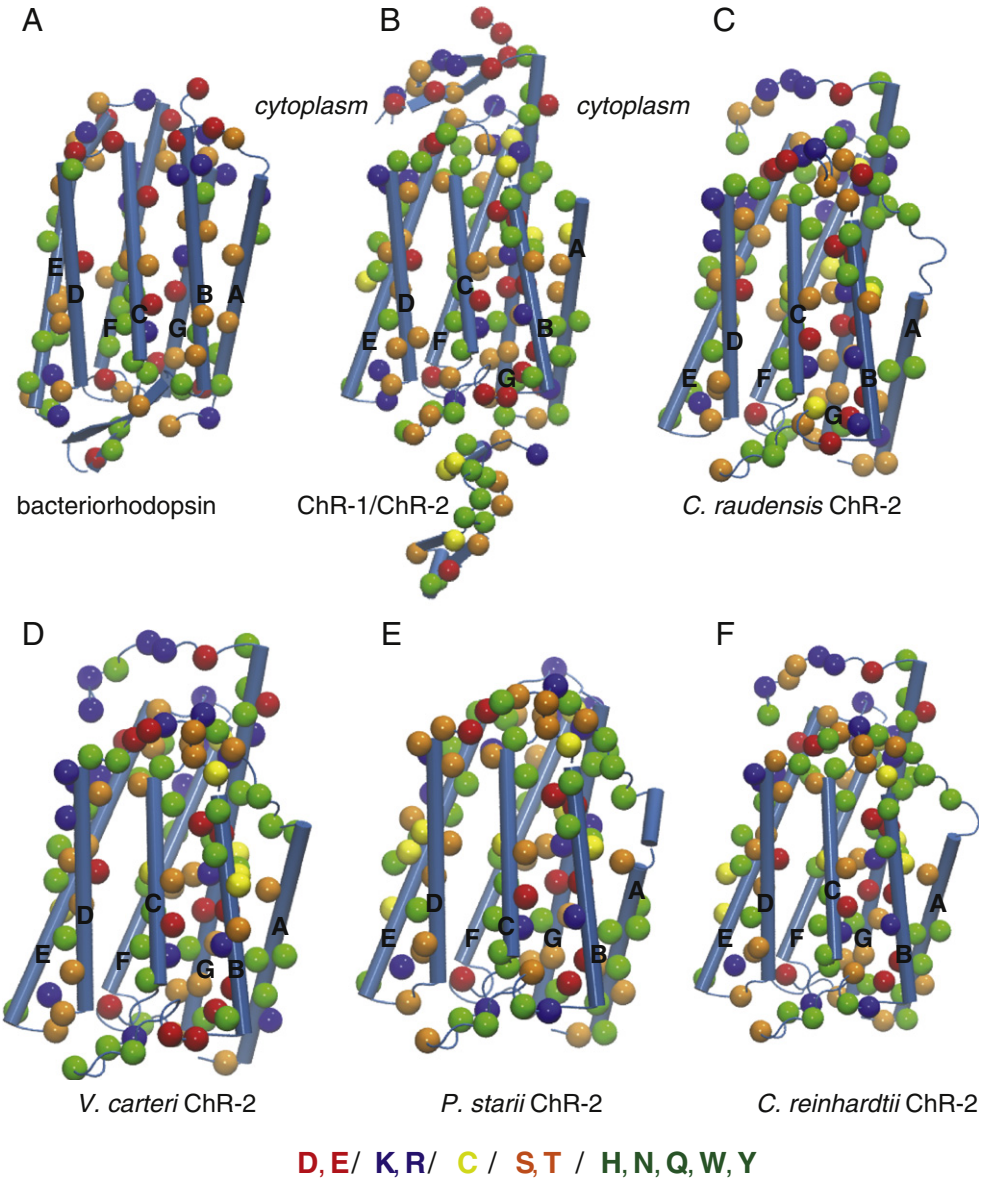

Fig. 3. Homology models of selected ChR-2 proteins illustrating the distribution of groups that can hydrogen bond. In panels A–G, the Cα atoms are shown as van der Waals spheres using the following color code: Ser/Thr — orange, Cys — yellow, Asn, Gln, His, Trp, Tyr — green, Asp/Glu — red, and Arg/Lys — blue. (A–B) The crystal structures of bacteriohodopsin [35] and the ChR1–ChR2 chimera [13] are shown as reference structures; the chimera structure was used as a template to generate the homology models depicted in panels C–F. Panels C–F give the three-dimensional homology-model structures of ChR-2 from, respectively, *C. raudensis*, *V. carteri*, *P. starii*, and *C. reinhardtii*. All molecular graphics images were prepared using VMD [105].

Compared to the proton-pumping BR, all channelrhodopsins from our dataset have more polar groups in helices B, C, D and G (Table 1, Figs. 1–4). Helix A also tends to be more polar, though for a few channelrhodopsins, such as *M. viride* ChR-1, the polarity of this helix is about the same as that for BR. Helix F is the least polar, and its overall polarity is, for most channelrhodopsins, less than half of that observed for BR; the larger hydrophobicity of helix F in channelrhodopsins as compared to BR is accompanied by a larger number of groups with small sidechains (Ala, Gly; see Figs. 1F and 2F) that could make helix F somewhat flexible. The charged groups are largely concentrated in helices B and G. Except for *C. yellowstonensis* ChR-1 and *C. augustae* ChR-1 that contain His, helix A of channelrhodopsins has no titratable group (Table 1b).

The increase in the percentage of polar groups of helix B in channelrhodopsins (~25–37%) relative to BR (17.4%) is largely due to the replacement of hydrophobic (I45, A53, M60, G63) or polar groups (T46) by Glu and, in most channelrhodopsins, also a Lys group (Figs. 1B and 2B). We denote as the helix B Glu motif the sequence EExxxxxxExxxxxxExxxX, where *x* is any amino acid. Of the channelrhodopsin sequences considered here, only *M. viride* ChR-1 and Pg ChR-1 do not have the helix B Glu motif (Fig. 1B). It has been suggested that the presence in *M. viride* ChR-1 of just three Glu groups in helix B (Fig. 1B) may explain the small currents measured for this channel [2]. It remains unclear why introducing in helix B the V102E/A116E mutation reduces the photocurrent [21].

In channelrhodopsins that have the helix-B Glu motif, the enhanced hydrophilicity of helix B is compensated in part by the replacement of BR T47 and S59 by a hydrophobic group (F, I, L or V). The Val at position 49 in BR is present in all channelrhodopsins, and is largely preceded by a Tyr group. All channelrhodopsins studied here have the helix-B Glu motif preceded by the sequence (C/T)GW. We can summarize these observations to refine the helix-B Glu motif of most channelrhodopsins to the sequence (GW)EE*b*YVx*b*Exx*b*ExxxE, where *b* is a hydrophobic group.

Within the refined helix-B Glu motif we note differences between ChR-1 and ChR-2. For example, in all ChR-2s studied here, the BR

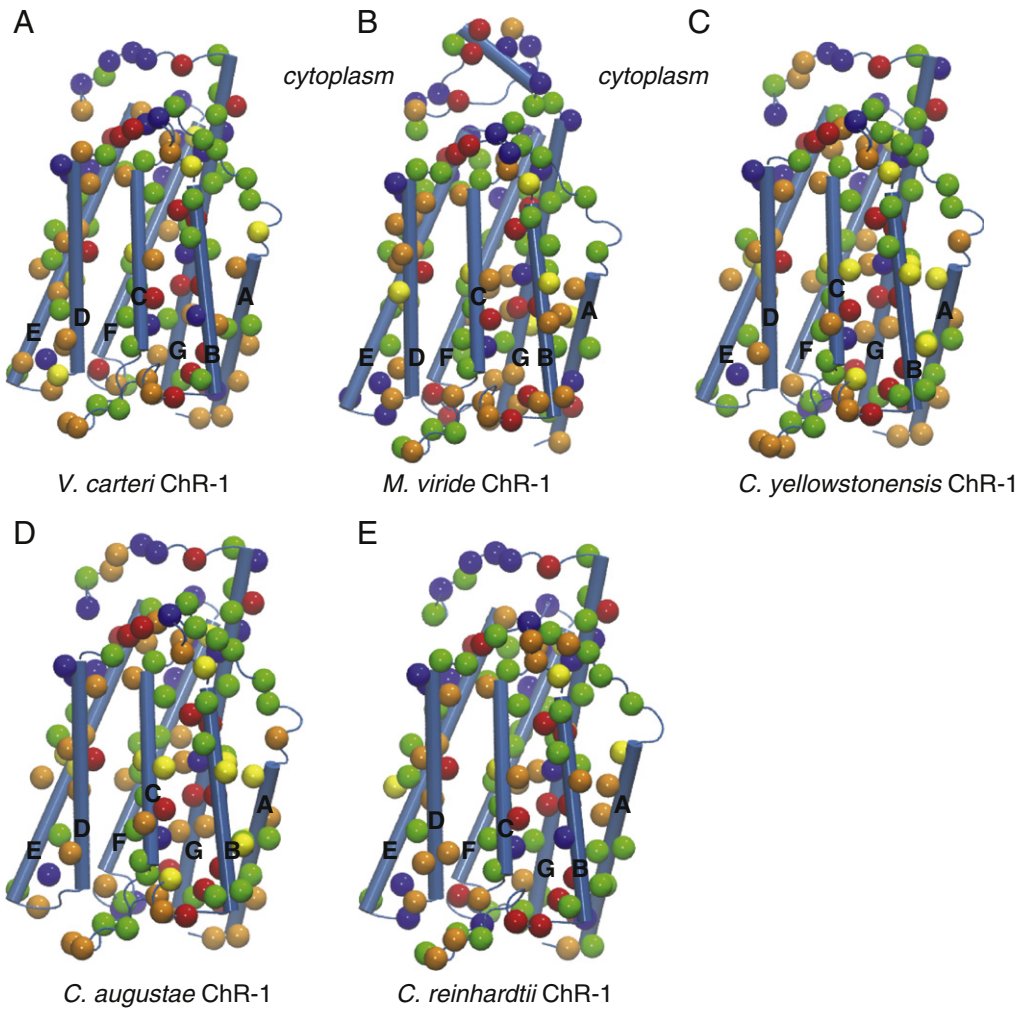

Fig. 4. Homology models of selected ChR-1 proteins illustrating the distribution of groups that can hydrogen bond. The color code for the amino acids is the same as in Fig. 3. Panels A–E illustrate the three-dimensional homology-structure models of ChR-1 from, respectively, *V. carteri*, *M. viride*, *C. yellowstonensis*, *C. augustae*, and *C. reinhardtii*.

amino acid residues P50, M56, and L62 are replaced by Cys, Lys and Phe respectively. ChR-1s tend to feature an insertion of a His/Ser in the position adjacent to the last Glu of the Glu motif, and the Lys close to the central Glu group is not necessarily present (Fig. 1B). With these additional observations, we can further restrict the Glu motif of ChR-2 to the sequence (GW)EE*b*YVCx*bEbx*KVx*bEbbx*E(F).

The details of how the transmembrane helices of channelrhodopsins are incorporated into the lipid membrane are not known. Since membrane insertion of peptides that contain polar and charged groups is energetically unfavorable [37,47,48], the significant polarity of helices B and G in channelrhodopsins (Table 1, Figs. 1–4) raises the question as to how the cellular machinery incorporates helices B and G into the membrane. When we subjected the sequences of the rhodopsin domains of *C. reinhardtii* ChR-2 and of the ChR-1/ChR-2 chimera to a translocon free energy of insertion analysis using MPeX with a window size of 20 amino acid residues (Membrane Protein Explorer, ref. [49]), MPeX predicted only five instead of seven transmembrane segments. In contrast, for BR MPeX correctly predicts seven transmembrane segments.

From experiments we know, for example, that inter-helical hydrogen bonds involving Asn, Asp, Gln, Glu and His can drive interactions between model transmembrane helices [50–52], that Asp-Asn and Asp-Asp pairs can promote the formation of helical hairpins [53], and that association of transmembrane helices can be facilitated by the presence of specific Ser/Thr motifs at the helix interface [54]. Given the spatial proximity of helices A–C and G (Figs. 3A and B) and the cooperativity observed for the folding of BR into lipids [55], we speculate that the membrane incorporation of helix B, which is loaded with charged and polar groups, may be facilitated by the possibility of hydrogen bonding between helices A–C and G: In channelrhodopsins, the increased hydrophilicity of helices C and G relative to BR (Table 1) is largely due to the replacement of hydrophobic groups by groups that can hydrogen bond (Figs. 1C and G and 2C and G). We note in particular the larger number of Cys, Ser, and Thr in helices A, C and D (Fig. 2C and D), and the increase in hydrogen-bonding groups of helix G (Fig. 2G). Protonation may also assist the membrane insertion of carboxylate-containing peptides [56].

Channelrhodopsins are not unique in that they have a transmembrane helix that is highly charged — another example is the voltage-sensing domain of the KvAP voltage-gated potassium channels, which has several Arg groups within the S4 transmembrane helical segment. Experiments demonstrated that the isolated S4 helix can be inserted into the lipid bilayer [57]; molecular dynamics simulations revealed that the lipid bilayer close to the peptide is thin, and that Arg groups can hydrogen bond to water and lipid phosphate groups [58]. The membrane interactions between the charged helix of channelrhodopsins and that of the KvAP voltage sensing domain

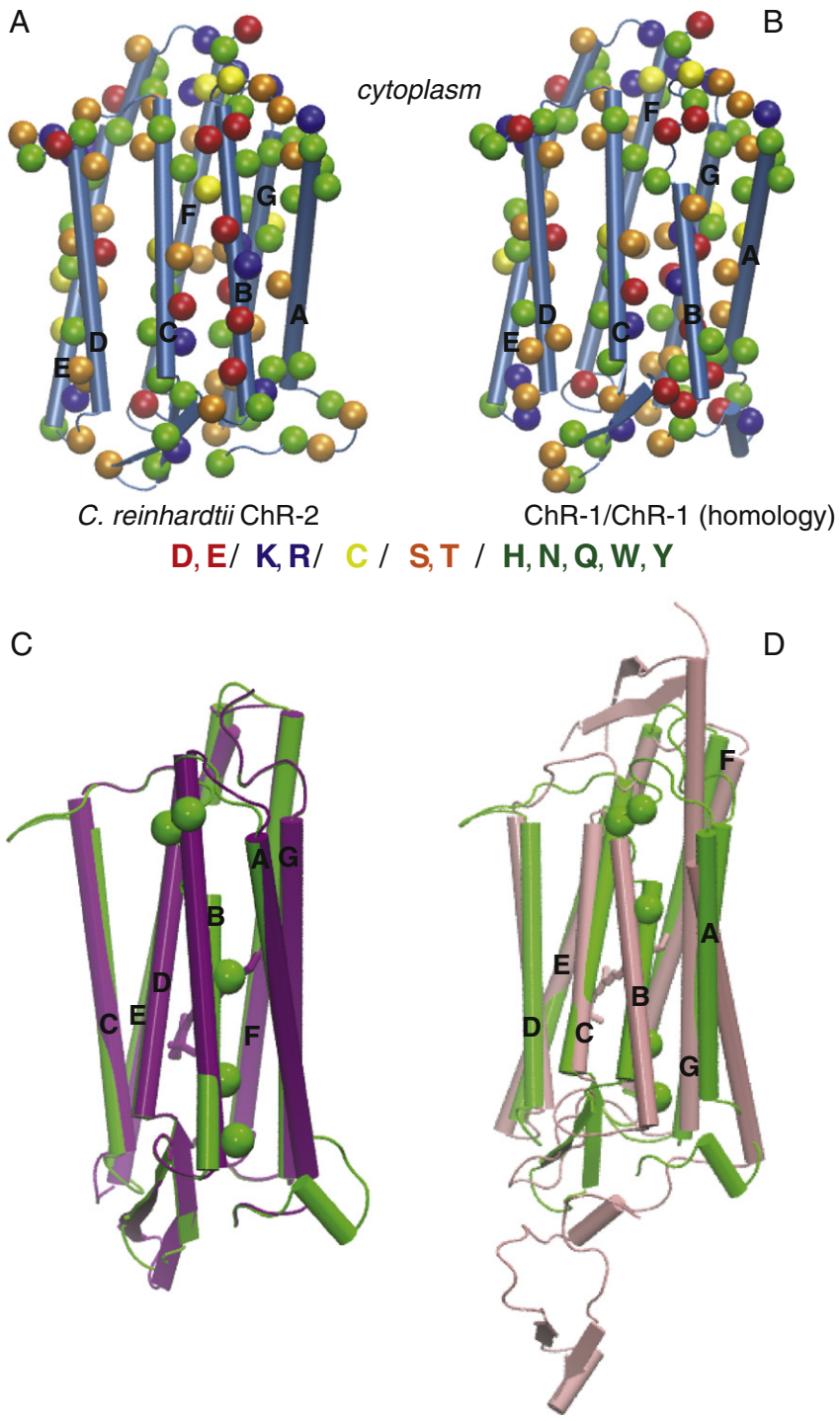

Fig. 5. Testing BR as a structure template for generating homology models of channelrhodopsins. (A) BR-based homology model of the rhodopsin domain of *C. reinhardtii* ChR-2 (compare to Fig. 3F). (B) BR-based homology model of the rhodopsin domain of the ChR-1/ChR-2 chimera (compare to Fig. 3B). (C) Comparison of the BR-based ChR-1/ChR-2 homology model with the BR crystal structure [35] used as a template. (D) Comparison of the BR-based ChR-1/ChR-2 homology model with the crystal structure of ChR-1/ChR-2 [13]. The overlaps from panels C and D were done using the SSM superpose tool of the Coot software [106] and depicted using VMD [105].

are, however, likely to be different: unlike the positively-charged Arg, Glu sidechains cannot hydrogen bond directly to lipid phosphate groups.

Our search for EExxxxxxExxxxxxExxxE motifs in other proteins led to hits indicating calcium, potassium, or sodium channels that contain Glu motifs (Fig. 6). Examples of EExxxxxxExxxxxxExxxE motifs found in other channels are the sequence EE*EEEEGQEGVEEEDEKDLE* of the *H. sapiens* voltage-dependent L-type calcium channel subunit alpha-1F isoform 1 (GenBank GI id 53832007), or the sequence EE*SNKEAKEEAELEAELELE* of the *H. sapiens* T-type calcium channel alpha 1G (GI ID 2921754).

Though the number of Glu groups and the separation between the Glu groups are the same as in the channelrhodopsin helix-B Glu motif, the hits obtained for other channels have signatures that are much more polar: The restricted channelrhodopsin helix-B Glu motif has at least four hydrophobic groups and a maximum of five carboxylates, whereas the other motifs we found via the database search have

Table 1
Polar and charged amino acid residues within the transmembrane helices.

a)

Sequence	Percentage of polar groups						
Helix	A	B	C	D	E	F	G
BR	10.0	17.4	21.7	18.2	13.6	23.8	26.1
ChR-1/ChR-2	22.0	33.3	30.4	36.4	18.2	9.5	34.8
V. carteri ChR-1	16.7	33.3	30.4	27.3	31.8	9.5	34.8
M. viride ChR-1	12.5	29.2	30.4	36.4	18.2	10.0	39.1
C. yellowstonensis ChR-1	22.2	25.0	34.8	27.3	18.2	14.3	39.1
C. augustae ChR-1	22.2	25.0	34.8	27.3	18.2	14.3	39.1
P. starii ChR-1	20.0	33.3	31.8	40.9	28.6	14.3	41.2
Pg ChR-1	12.5	25.0	26.1	36.4	18.2	9.5	34.8
C. reinhardtii ChR-1	22.2	33.3	30.4	36.4	18.2	9.5	39.1
C. raudensis ChR-2	11.1	37.5	30.4	36.4	31.8	9.5	43.5
V. carteri ChR-2	16.7	33.3	30.4	36.4	22.7	9.5	39.1
P. starii ChR-2	21.1	25.0	34.8	27.3	25.0	9.5	39.1
C. reinhardtii ChR-2	16.7	25.0	34.8	31.8	22.7	9.5	34.8

b)

Sequence	Percentage of charged amino acid residues						
Helix	A	B	C	D	E	F	G
BR	0.0	0.0	13.0	4.5	4.5	9.5	17.4
ChR-1/ChR-2	0.0	29.2	13.0	9.1	9.1	0.0	21.7
V. carteri ChR-1	0.0	29.2	13.0	9.1	13.6	4.8	21.7
M. viride ChR-1	0.0	12.5	8.7	9.1	4.5	4.8	26.1
C. yellowstonensis ChR-1	5.6	25.0	13.0	9.1	9.1	4.8	21.7
C. augustae ChR-1	5.6	25.0	13.0	9.1	9.1	4.8	21.7
P. starii ChR-1	0.0	33.3	13.6	9.1	14.3	4.8	23.5
Pg ChR-1	0.0	12.0	8.7	13.6	9.1	0.0	17.4
C. reinhardtii ChR-1	0.0	29.2	13.0	9.1	9.1	4.8	26.1
C. raudensis ChR-2	0.0	29.2	13.0	13.6	13.6	4.8	26.1
V. carteri ChR-2	0.0	29.2	13.0	13.6	13.6	4.8	26.1
P. starii ChR-2	0	25	13.0	4.5	10	0	26.1
C. reinhardtii ChR-2	0	25	13.0	4.5	13.63	0	21.7

a) Composition of the polar amino acid residues, as percentage of each helix. As polar amino acid residues we counted D, E, H, K, N, Q, R, S, and T.
b) Composition of the amino acid residues that can have a net charge. We counted here D, E, H, K and R.

fewer hydrophobic groups and more charged or other polar groups (Fig. 6) that are most likely solvent-exposed. That is, based on the current database search, we could not find another class of channels that has a sequence fragment qualitatively similar to that of the helix-B Glu motif.

Understanding the context in which polar Glu-rich motifs may appear in other channels would require information on the three-dimensional structure of these proteins. Since our search of the helix B Glu motif using the database of known protein structures PDB_TM (ref. [39]; version 2013-06-07) returned the ChR-1/ChR-2 chimera structure [13] as the only hit, at the moment channelrhodopsins appear as the only membrane proteins with a helix B Glu motif for which we have information on the three-dimensional structure.

Table 2
Summary of homology models for the rhodopsin domain of selected channelrhodopsins.

Sequence	Sequence length	Template used[a]	Sequence identity (%)[b]
V. carteri ChR-1	G39-I284	ChR-1/ChR2	67
M. viride ChR-1	G65-G324		41
C. yelowstonesis ChR.1	G91-I336		55
C. augustae ChR-1	G90-I335		55
C. reinhardtii ChR-1	G83-V328		85
C. raudensis ChR-2	G88-V333		63
V. carteri ChR-2	G39-V284		72
P. starii ChR-2	P1-V227		68
C. reinhardtii ChR-2	G44-I289		79
C. reinhardtii ChR-2		BR	16
ChR-1/ChR-2[c]	G60-I305		17

[a] For the template structure we used the ChR-1/ChR-2 structure from ref. [13] or the BR structure from ref. [35].
[b] The sequence identity between each query sequence and the template is given as indicated by Phyre2 [46].
[c] We derived a homology model of the chimera structure based on BR as a template to check it against the true crystal structure from ref. [13].

6. Conservation motifs of transmembrane helical segments

Close inspection of the sequence alignments reveals that, within the dataset considered here, there are highly conserved motifs shared by the putative transmembrane segments of channelrhodopsins (Fig. 1, Table 3). We find that some of the conserved motifs are present in all channelrhodopsins, whereas others appear mostly in one type of proteins (Table 3). In what follows we discuss the changes in the sequences of amino acids that encompass three carboxylates critical for proton transport in BR (D85, D115, and D212); these carboxylates are part of helices C, D, and G, respectively.

The sequence of helix C is highly conserved among channelrhodopsins (Fig. 1C). Significant differences in the sequences of helix C in BR vs. channelrhodopsins are at the D85 and D96 proton transfer sites of BR (Fig. 1C, Table 3). The importance of the replacement of D85 by Glu is illustrated by site-directed mutagenesis experiments on the both BR and channelrhodopsins. In BR, the D85E mutation is associated with faster deprotonation of the retinal [59–64], since the longer Glu sidechain is more flexible than Asp [63,64]. In the closed state of the ChR-1/ChR-2 chimera, the Glu replacing BR D85 (E162, Fig. 7C) might be protonated [13], and replacing by Thr the corresponding Glu in *C. reinhardtii* (E123) changes the equilibrium between two open states of the protein [4]. Given the complexity of the environment in the vicinity of E162 (Fig. 7C), and our observations on changes in protein dynamics when hydrogen bonds are affected [65], we suggest that understanding the E123 mutations would require studies of protein dynamics.

At the BR proton donor site, the D_{96}LALLV sequence is replaced, in almost all channelrhodopsin sequences, by HLSNLT (Fig. 1C). That is, one carboxylate and three hydrophobic groups are replaced by four groups that can hydrogen bond. As discussed below in Section 7, we think that these changes in hydrogen bonding can have important consequences for the local structure, dynamics, and hydration of helix C. The importance of the context of the amino acid sequence at the BR D96 site is further illustrated by observations from experiments that, in ChR-2, mutation to Arg of the His replacing BR D96 affects the conductance of sodium ions [2,7]; replacing the His back into Asp, that is, recovering the BR D96 proton donor, led to loss of the light-gated conductance in *C. reinhardtii* ChR-1 [5]. In *M. viride* ChR-1, D96 is replaced by Ala (A153 in Fig. 1C), and mutation of this group to His or Arg suppresses the current [21].

D115 of helix D is present in all channelrhodopsins, except for *P. starii* ChR2 where it is replaced by Ser (Fig. 1D). But the amino acids adjacent to D115 (D156 in *C. reinhardtii* ChR-2) are different in BR vs. channelrhodopsins. In BR, the amino acid residues neighboring D115 within helix D have small sidechains — Ala and Gly. In channelrhodopsins, the ADG sequence is mostly replaced by SDx, where *x* is either Val or Ile (Fig. 1D). The changes in the sequence of helix D are accompanied by changes in hydrogen bonding between helices D and C: Whereas in BR D115 hydrogen bonds to T90, in channelrhodopsins T90 is always replaced by Cys (C128 in *C. reinhardtii* ChR-2, and C167 in ChR-1/ChR-2, Fig. 7C). In spite of these changes in the amino acid sequences, it is thought that a hydrogen bond is present between helix-C Cys and helix-D Asp of *C. reinhardtii* ChR-2 [66]; the Asp/Cys interaction appears important for the reaction cycle of the channel, because mutation of C128 back into Thr affects the timescale of conformational changes [19]. The changes in the sequences of helices C and D at the site of the interhelical hydrogen bond may be related to the different roles of the Asp: whereas in BR D115 remains protonated throughout the reaction cycle [67], the corresponding D156 of ChR2 deprotonates, and is thought to be the internal proton donor for the retinal Schiff base [12].

Replacement of helix-G D212 greatly affects the reaction cycle of BR (e.g., ref. [40]). Though D212 is present in all channelrhodopsins studied

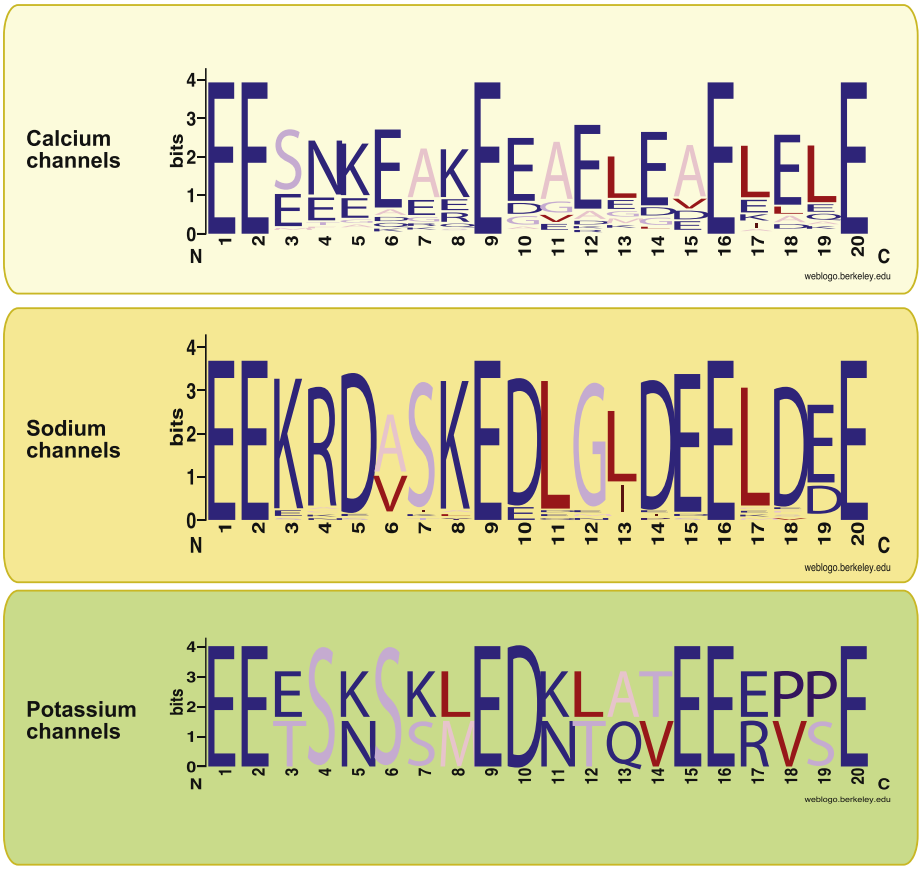

Fig. 6. Sequence logos illustrating the results of the database search for EExxxxxxExxxxxxExxxE motifs. Although five-glutamate motifs were found in other channels, within the dataset used we could not find other channels having the more restrictive Glu motif of helix B observed in channelrhodopsins (EE*b*YVx*b*Exx*b*ExxxE, where *b* is a hydrophobic group).

here, the sequence context in which the Asp is found is different from that of BR: immediately upstream the sequence the Asp is separated from a Ser by one amino acid in BR, vs. two amino acids in channelrhodopsins (Fig. 1G, Table 3). This change in the position of the Ser relative to the Asp group is important, because Ser sidechains can hydrogen bond to the backbone amide groups and influence the local dynamics of the helix (see discussion in Section 7 below).

The environment of D212 is changed not only within helix G, but also in its inter-helical hydrogen bonding. In BR D212 hydrogen bonds to Y57 and Y185, and mutation of either Tyr to Phe affects the reaction cycle: The Y57F mutation affects the order of proton release and uptake [68], and Y185F appears to stabilize a late intermediate of the reaction cycle [69]. The ChR-1/ChR-2 crystal structure indicates Phe groups at the positions corresponding to Y57 and Y185 (Fig. 7C), suggesting that inter-helical coupling between helices B, F and G at the D212 site (D292 in ChR-1/ChR-2) is weaker in channelrhodopsins than in BR.

Table 3
Illustration of common sequence conservation patterns.

Helix	Sequence motif	ChR-1	ChR-2
A	$Q_{56}W_{57}$	+	+
	Y_{71}	+	+
B	CGWEE*b*YVx*b*Exx*b*ExxxE	+	+
	CGWEE*b*YVCx*b*E*b*xKVx*b*E*bb*xEF	−	+
C	$T_{127}C_{128}$[a]	+	+
	H_{134}LSNLT_{139}	+	+
D	R_{148}TMxLLxx_1Dxx_2x_3 [a,b]	+	+
E	K_{174}xxFx$_4$xxG_{181}[c]	+	+
	Y_{184}xxNTxxxxA_{193}[d]	−	+
F	$V_{212}x_5xx_6A_{216}$[e]	+	+
G	D_{253}xxSKN_{258}	+	+

The numbers in subscripts refer to the sequence of *C. reinhardtii* ChR-2. *x* denotes any amino acid residue, and *b* denotes a hydrophobic group.

[a] The entire helix C has significant conservation among channelrhodopsins (see the main text).

[b] x_1 is mostly Ser; x_2 is always Gly in ChR-2, and Gly, Ala or Cys in ChR-1; x_3 is either Thr or Cys (Fig. 1D).

[c] x_4 is always Phe in ChR-2, and either Phe or Tyr in ChR-1.

[d] The Asn of this motif is often replaced by Tyr in ChR-1.

[e] x_5 is Arg, Lys, Ser, or Thr; x_6 is either Met (in all type-2 channelrhodopsins) or Leu.

7. The Cys/Ser/Thr motifs of channelrhodopsins

Analysis of the composition of the amino acids of the transmembrane helical segments of channelrhodopsins reveals an increase in the total number of Cys, Ser, and Thr groups relative to BR (Figs. 2, 3, and 4). This increase is largely due to the Cys groups — whereas BR has no Cys group, the putative transmembrane segments of channelrhodopsins have between four (e.g., *C. raudensis* ChR-1) and ten Cys groups (e.g., *C. augustae* ChR-1). The Cys groups are mostly present in helices B and C. The channelrhodopsins considered here have multiple Ser/Thr groups within helix D; moreover, within helix D there is significant conservation of Ser/Thr in the positions corresponding to BR I108, A114, M118, V124 and, to some extent, G125 and T128 (Fig. 1D). Helix C contains a highly conserved TC motif corresponding to BR T89 and T90; in *C. yellowstonensis* and *C. augustae* ChR-1, the TC motif of helic C is replaced by CC (Figs. 1C, 4C and D). Some of the Cys/Ser/Thr groups are clustered approximately at the middle of the putative pore (see, e.g., Figs. 3B and D, 4D and E, and7A).

The presence of multiple Ser and Thr groups within the transmembrane helices of channelrhodopsins is intriguing, because experiments indicate positive free energies of insertion in the membrane hydrophobic core [48,70]. Consistent with these observations from experiments,

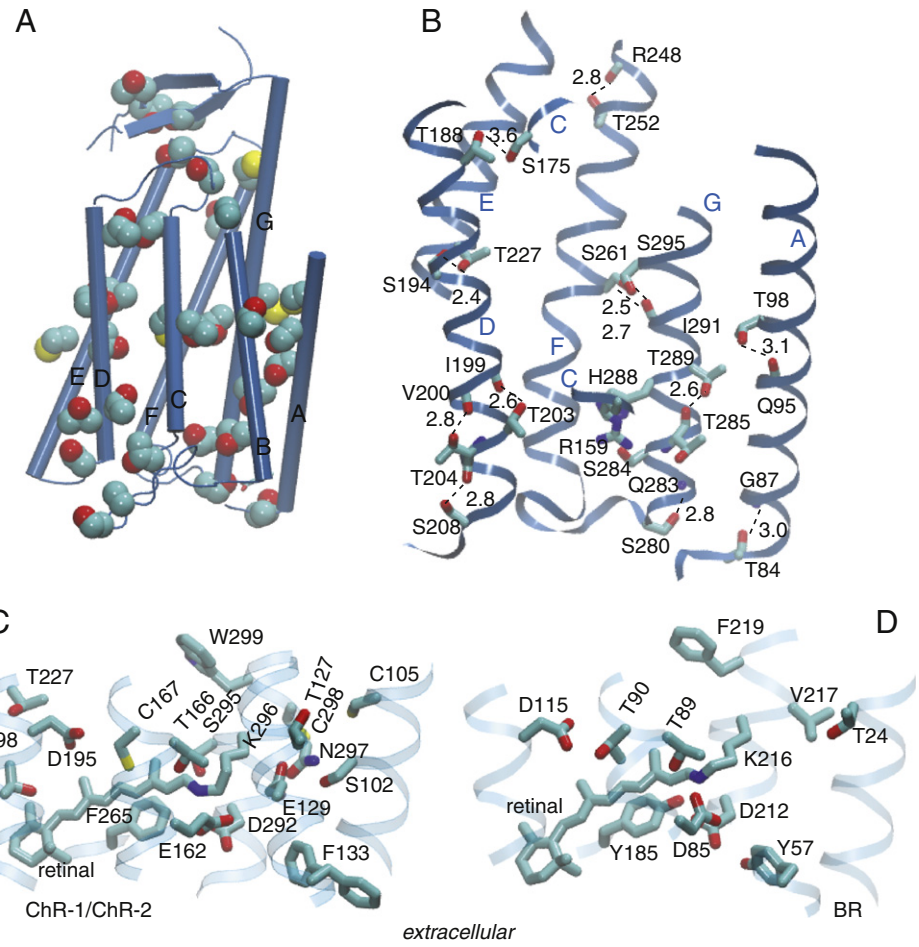

Fig. 7. The Ser and Thr groups mediate inter- and intra-helical hydrogen bonds. (A) Distribution of Cys, Ser and Thr in the chimera structure ChR-1/ChR-2. Panels A–C are based on the crystal structure from ref. [13]. Note the higher density of such groups at approximately the middle of the protein, and between helices A and G. (B) Illustration of hydrogen bonds mediated by Ser and Thr groups. For clarity, we show only those small portions of helix C that include R159 and S175. The broken lines indicate hydrogen bonds; the numbers close to the broken lines give the distance between the hydrogen bond donor and acceptor heavy atoms. Note that helix D has three intra-helical hydrogen bonds, and two inter-helical hydrogen bonds that involve Ser/Thr. (C) Selected charged and polar groups close to the retinal chromophore in the ChR-1/ChR-2 chimera. (D) Selected charged and polar groups close to the retinal chromophore in the BR structure from ref. [35].

the likelihood of finding Ser/Thr at the middle of α-helices is small [71], and the probability of finding two Ser groups within the same transmembrane helix is low, ~20% [72]. Our previous bioinformatics analyses of membrane proteins containing α-helical transmembrane segments indicated that 45–58% of the proteins do not contain multiple Ser/Thr groups [73]. We did, however, identify α-helical membrane proteins that have numerous Ser/Thr groups, in particular transporters and receptors [73].

An important aspect concerning Ser/Thr in membrane proteins is that their hydroxyl groups can have both inter- and intra-helical hydrogen bonds. In what the inter-helical hydrogen bonds are concerned, we know that Ser/Thr motifs can promote helix interaction via hydrogen bonding [54,74]. The intra-helical hydrogen bonds of Ser/Thr are formed via the interaction of their hydroxyl group with backbone amide or carbonyl groups [71,73,75–80]. Intra-helical hydrogen bonding of the hydroxyl group of a Ser/Thr group to the amide group of the *i-4* amino acid residue is associated with an enhanced local dynamics of the helix; depending on the sequence context, the presence of multiple Ser groups within a transmembrane helix can also be associated with an enhanced local hydration [73].

The crystal structure of the ChR-1/ChR-2 chimera [13] indicates both inter- and intra-helical hydrogen bonds mediated by Ser and Thr (Fig. 7). Helices D and E are bridged by a short-distance hydrogen bond (2.4 Å) between S194 and T227 (Fig. 7B). Both helix-F S261 and helix-G S295 hydrogen bond to the carbonyl group of helix-G I291. The Ser/Thr groups of helix D engage in three hydrogen bonds with the *i-4* backbone carbonyls (T203, T204, and S208 in Fig. 6B), and two hydrogen bonds with helices C and G (S194 and T188 in Fig. 7B). Inspection of the homology model structures of several ChR-1s (Figs. 4C–E) and ChR-2s (Fig. 3D and F) suggests that, within the accuracy of a homology model, helix D tends to have both intra-helical and inter-helical hydrogen bonds. A network of hydrogen bonds involving Ser/Thr groups of helices D and E was also noted in a homology model of *Dunaliella salina* ChR-2 [27].

Based on our previous simulations on model peptides containing Ser/Thr [73], we hypothesize that the intra- and inter-helical hydrogen bonds of helix D are important structural determinants of the dynamics of the helix. The dynamics of helix D are likely important for the channel function, because helix D contains the conserved Asp (D115 in BR) that hydrogen bonds to a Thr on helix C (BR T90, see Fig. 7D). The reason why BR T90 is replaced by Cys in all channelrhodopsins studied here is not clear (Fig. 1C; see C167 in Fig. 7C). FTIR spectroscopy experiments indicate a hydrogen bond between the corresponding Asp and Cys of *C. reinhardtii* ChR-2 [66]. The distance between the sidechains of D195 and C167 in the ChR-1/ChR-2 crystal structure (4.5 Å, see Fig. 7C) is somewhat large for a hydrogen bond [13], and molecular dynamics simulations were interpreted to suggest that the Asp/Cys hydrogen bond between helices C and D may be mediated by water [81,82]. Though indeed hydrogen bonding of a cysteine sidechain is weaker than that of a hydroxyl group [83] and may be dynamic, we note here that the

crystal structure of *Acetabularia acetabulum* rhodopsin [84] offers another example of a carboxylate/sulfydryl inter-helical interaction; the Asp and Cys groups of *A. acetabulum* rhodopsin correspond to, respectively, D96 and L223 of BR (Fig. 1B,C). High-resolution crystal structures and prolonged molecular dynamics simulations of wild-type channelrhodopsin intermediate states would be necessary to dissect the structural and dynamical determinants of the spectral fingerprints observed in experiments.

8. Implications for water dynamics and the proton-transfer mechanism

The availability of the crystal structure of the ChR-1/ChR-2 chimera [13] and information from spectroscopy regarding the protonation states along the reaction cycle of, e.g., *C. reinhardtii* ChR-2 [12] provide starting points for computations of putative proton-transfer pathways, though differences in the electrical currents recorded for various channelrhodopsin [16] suggest that structures of wild-type channelrhodopsins may be necessary for comparing experiments and computations.

The essential role of waters in proton pumping by BR (see, e.g., refs. [85–97]) highlights the importance of accurate information on how water dynamics couple to the protonation/deprotonation reactions and to ion transfer in channelrhodopsins. The polar environment of the putative ion-conducting pore is compatible with waters being present inside channelrhodopsin — as molecular dynamics simulations also appear to suggest (e.g., refs. [11,24,82]). The higher polarity of the retinal Schiff base environment in channelrhodopsins vs. BR (Figs. 5A, B, and 7C, D) could imply different energetics for water motions in the retinal region: In BR, hydrophobic groups close to the K216 sidechain contribute to the rate-limiting step for the passage of a water molecule on the D212 side of the retinal (Fig. 7D) [98]. Replacement of A215 by Ser and of the hydrophobic $V_{217}GF_{219}$ sequence by NxW in most channelrhodopsins (Figs. 1G, 7C and D) is likely to alter the energetics of water movement in the retinal Schiff base region.

The numerous polar and charged groups of the transmembrane helical segments (Figs. 1–3, 7B, Table 1) could give rise to complex hydrogen-bond dynamics, as we indeed observed for other membrane proteins [65,99,100]. The importance of dynamical inter-helical hydrogen bonds for the conformational dynamics of the protein [100] and the large extent to which protein dynamics can couple to the protonation state [101] highlight the importance of accurate protein structures, and raise the questions as to how inter-helical hydrogen bonds involving inter-helical polar and charged groups (Figs. 1, 3 and 4) affect the dynamics of channelrhodopsin, and how the protein and water dynamics couple to proton transfers.

9. Conclusions

We performed bioinformatics analyses of channelrhodopsins and inspected conservation motifs. Within the set of sequences analyzed here, we find that some conservation patterns are observed in all channelrhodopsins, whereas others appear specific to ChR-1 or to ChR-2. For example, though most channelrhodopsins have five Glu groups in helix B, the signature of the helix-B Glu motif appears somewhat more restricted in ChR-2 than in ChR-1 (Table 3). Likewise, the Asp of helix D (D156 in *C. reinhardtii* ChR-2) appears always in the context DxG when in ChR-2, but in ChR-1 the Gly upstream the Asp can be replaced by Ala or Cys (Fig. 1D).

Dynamic inter-helical hydrogen bonds can influence the conformational equilibrium of a membrane protein [100]. An interaction that appears particularly important for the conformational dynamics of channelrhodopsin is between a helix-C Asp and a helix-D Cys group, at the site of the so-called DC gate [66]. The relevance of this interaction for understanding the conformational dynamics of channelrhodopsins is underscored by the observations that, in ChR-2 the C128T mutation changes the kinetics of the reaction cycle [19]. Based on the analysis of the sequences considered here, and considering the significant effects that the presence of multiple Ser/Thr groups can have on the dynamics of a transmembrane helix [73], we suggest that the dynamics of helices C and D along the channelrhodopsin reaction cycle may be very different from BR. Recent experiments suggest that helices B and F move during the reaction cycle [102,103]. Given the spatial proximity between helices B and C (e.g., Figs. 3B and 7A) and that helix B contains many groups that can hydrogen bond (Fig. 1A), movement of helix B may be coupled to rearrangements of inter-helical hydrogen bonds and changes of protein and water dynamics at remote sites in the protein. The numerous charged and polar groups of the transmembrane region of channelrhodopsins (Figs. 3, 4, and 7A–B) could give rise to complex patterns of inter-helical hydrogen bonding networks, and participate in coupling the dynamics of the protein to its protonation state.

Acknowledgements

This research was supported in part by the Spanish Ministerio de Ciencia e Innovación (project TIN2012-38805), the Consejería de Innovación, Investigación y Ciencia de la Junta deAndalucía (project TIC-02788) and the GENIL program (PYR-2010-28) to CdV, and by the Marie Curie International Reintegration Award IRG-276920 and the Deutsche Forschungsgemeinschaft, Collaborative Research Center SFB 1078, Project C4, to A-NB.

Appendix A. Supplementary data

Supplementary data to this article can be found online at http://dx.doi.org/10.1016/j.bbabio.2013.11.005.

References

[1] L. Petreanu, D. Huber, A. Sobczyk, K. Svoboda, Channelrhodopsin-2-assisted circuit mapping of long-range callosal projections, Nat. Neurosci. 10 (2007) 663–668.
[2] F. Zhang, J. Vierock, O. Yizhar, L.E. Fenno, S. Tsunoda, A. Kianianmomeni, M. Prigge, A. Berndt, J. Cushman, J. Polle, J. Magnuson, P. Hegemann, K. Deisseroth, The microbial opsin family of optogenetic tools, Cell 147 (2011) 1446–1457.
[3] P. Hegemann, G. Nagel, From channelrhodopsins to optogenetics, EMBO Mol. Med. 5 (2013) 173–176.
[4] L.A. Gunaydin, O. Yizhar, A. Berndt, V.S. Sohal, K. Deisseroth, P. Hegemann, Ultrafast optogenetic control, Nat. Neurosci. 13 (2010) 387–392.
[5] G. Nagel, D. Ollig, M. Fuhrmann, S. Kateriya, A.M. Musti, E. Bamberg, P. Hegemann, Channelrhodopsin-1: a light-gated proton channel in green algae, Science 296 (2002) 2395–2398.
[6] G. Nagel, T. Szellas, S. Kateriya, N. Adeishvili, P. Hegemann, E. Bamberg, Channelrhodopsins: directly light-gated cation channels, Biochem. Soc. Trans. 33 (2005) 863–866.
[7] G. Nagel, M. Brauner, J.F. Liewald, N. Adeishvili, E. Bamberg, A. Gooschalk, Light activation of channelrhodopsin-2 in excitable cells of *Caenorhabditis elegans* triggers rapid behavioral response, Curr. Biol. 15 (2005) 2279–2284.
[8] M. Nack, I. Radu, C. Bamann, E. Bamberg, J. Heberle, The retinal structure of channelrhodopsin-2 assessed by resonance Raman spectroscopy, FEBS Lett. 583 (2009) 3676–3680.
[9] I. Radu, C. Bamann, M. Nack, G. Nagel, E. Bamberg, J. Heberle, Conformational changes of channelrhodopsin-2, J. Am. Chem. Soc. 131 (2009) 7313–7319.
[10] E. Ritter, K. Stehfest, A. Berndt, P. Hegemann, F. Bartl, Monitoring light-induced structural changes of channelrhodopsin-2 by UV-visible and Fourier transform infrared spectroscopy, J. Biol. Chem. 283 (2008) 350033-35041.
[11] K. Eisenhauer, J. Kuhne, E. Ritter, A. Berndt, S. Wolf, E. Freier, F. Bartl, P. Hegemann, K. Gerwert, In channelrhodopsin-2 Glu-90 is crucial for ion selectivity and is deprotonated during the photocycle, J. Biol. Chem. 287 (2012) 6904–6911.
[12] V.A. Lórenz-Fonfria, T. Resler, N. Krause, M. Nack, M. Gossing, G. Fischer von Mollard, C. Bamann, E. Bamberg, R. Schlesinger, J. Heberle, Transient protonation changes in channelrhodopsin-2 and their relevance to channel gating, Proc. Natl. Acad. Sci. U. S. A. 110 (2013) E1273–E1281.
[13] H.E. Kato, F. Zhang, O. Yizhar, C. Ramakrishnan, T. Nishizawa, K. Hirata, J. Ito, Y. Aita, T. Tsukazaki, S. Hayashi, P. Hegemann, A.D. Maturana, R. Ishitani, K. Deisseroth, O. Nureki, Crystal structure of the channelrhodopsin light-gated cation channel, Nature 482 (2012) 369–374.
[14] D.C. Gadsby, Ion channels versus ion pumps: the principal difference, in principle, Nat. Rev. Mol. Cell Biol. 10 (2009) 344–352.
[15] L.S. Brown, The thin line between channels and pumps, Biophys. J. 104 (2013) 739–740.
[16] O.A. Sineschchekov, E.G. Govorunova, J. Wang, H. Li, J.L. Spudich, Intramolecular proton transfer in channelrhodopsin, Biophys. J. 104 (2013) 807–817.

[17] K. Feldbauer, D. Zimmermann, V. Pintschovius, J. Spitz, C. Bamann, E. Bamberg, Channelrhodopsin-2 is a leaky proton pump, PNAS 28 (2009) 12317–12322.
[18] K. Stehfest, E. Ritter, A. Berndt, F. Bartl, P. Hegemann, The branched photocycle of the slow-cycling channelrhodopsin-2 mutant C128T, J. Mol. Biol. 398 (2010) 690–702.
[19] C. Bamann, R. Gueta, S. Kleinlogel, G. Nagel, E. Bamberg, Structural guidance of the photocycle of channelrhodopsin-2 by an interhelical hydrogen bond, Biochemistry 49 (2010) 267–278.
[20] A. Berndt, P. Schoeneberger, J. Mattis, K.M. Tye, K. Deisseroth, P. Hegemann, T.G. Oerther, High-efficiency channelrhodopsins for fats neuronal stimulation at low light levels, Proc. Natl. Acad. Sci. U. S. A. 108 (2011) 7595–7600.
[21] E.G. Govorunova, E.N. Spudich, C.E. Lane, O.A. Sineshchekov, J.L. Spudich, New channelrhodopsins with a red-shifted spectrum and rapid kinetics from *Mesostigma viride*, mBio 2 (2011) e00115-11, 1–9.
[22] D. Gradmann, A. Berndt, F. Schneider, P. Hegemann, Rectification of the channelrhodopsin early conductance, Biophys. J. 101 (2011) 1057–1068.
[23] J.Y. Lin, M.Z. Lin, P. Steinbach, R.Y. Tsien, Characterization of engineered channelrhodopsin variants with improved properties and kinetics, Biophys. J. 96 (2009) 1803–1814.
[24] A.P. Plazzo, N. de Franceschi, F. da Broi, F. Zonta, M.F. Sanasi, F. Filippini, M. Mongillo, Bioinformatic and mutational analysis of channelrhodopsin-2 cation conductance pathway, J. Biol. Chem. 287 (2012) 4818–4825.
[25] R. Richards, R.E. Dempski, Re-introduction of transmembrane serine residues reduce the minimum pore diameter of channelrhodopsin-2, PLoS One 7 (2012) e50018.
[26] M. Müller, C. Bamann, E. Bamberg, W. Kühlbrandt, Projection structure of channelrhodopsin-2 at 6 Å resolution by electron crystallography, J. Mol. Biol. 414 (2011) 86–95.
[27] H. Watanabe, K. Welke, F. Schneider, S. Tsunoda, F. Zhang, K. Deisseroth, P. Hegemann, M. Elstner, Structural model of channelrhodopsin, J. Biol. Chem. 287 (2012) 7456–7466.
[28] J.D. Thomson, J.D. Gibson, D.G. Higgins, Multiple sequence alignment using ClustalW and ClustalX, Curr. Protoc. Bioinforma. (2002)(Chapter 2, Unit 2.3). http://dx.doi.org/10.1002/0471250953.bi0203s00.
[29] K. Katoh, H. Toh, Recent developments in the MAFFT multiple sequence alignment program, Brief Bioinform. 9 (2008) 286–298.
[30] R.C. Edgar, MUSCLE: multiple sequence alignment with high accuracy and high throughput, Nucleic Acids Res. 32 (2004) 1792–1797.
[31] C. Notredame, D.G. Higgins, J. Heringa, T-Coffee: a novel method for fast and accurate multiple sequence alignment, J. Mol. Biol. 302 (2000) 205–217.
[32] P. Hogeweg, B. Hesper, The alignment of sets of sequences and the construction of phyletic trees: An integrated method, J. Mol. Evol. 20 (1984) 175–186.
[33] G. Blackshields, I.M. Wallace, M. Larkin, D.G. Higgins, Analysis and comparison of benchmarks for multiple sequence alignment, In Silico Biol. 6 (2006) 321–339.
[34] C. Notredame, Recent evolutions of multiple sequence alignment algorithms, PLoS Comput. Biol. 3 (2007) e123.
[35] H. Belrhali, P. Nollert, A. Royant, C. Menzel, J.P. Rosenbusch, E.M. Landau, E. Pebay-Peyroula, Protein, lipid and water organization in bacteriorhodopsin crystals: a molecular view of the purple membrane at 1.9 Å resolution, Structure 7 (1999) 909–917.
[36] H.M. Berman, K. Henrick, H. Nakamura, Announcing the worldwide Protein Data Bank, Nat. Struct. Biol. 10 (2003) 980.
[37] T. Hessa, H. Kim, K. Bihlmaier, C. Lundin, J. Boekel, H. Andersson, I. Nilsson, S.H. White, G. von Heijne, Recognition of transmembrane helices by the endoplasmic reticulum translocon, Nature 433 (2005) 377–381.
[38] P. Rice, I. Longden, A. Bleasby, EMBOSS: The European Molecular Biology Open Software Suite, Trends Genet. 16 (2000) 276–277.
[39] G.E. Tusnady, Z.S. Dosztanyi, I. Simon, PDB_TM: selection and membrane localization of transmembrane proteins in the protein data bank, Nucleic Acids Res. 33 (2005) D275–D278.
[40] Y. Huang, B. Niu, Y. Gao, L. Fu, W. Li, CD-HIT Suite: a web server for clustering and comparing biological sequences, Bioinformatics 26 (2010) 680–682.
[41] T.D. Schneider, G.D. Stormo, L. Gold, A. Ehrenfeucht, Information content of binding sites on nucleotide sequences, J. Mol. Biol. 188 (1986) 415–431.
G.E. Crooks, G. Hon, J.-M. Chandonia, S.E. Brenner, WebLogo: a sequence logo generator, Genome Res. 14 (2004) 1188–1190.
[42] M.A. Martí-Renom, A.C. Stuart, A. Fiser, R. Sánchez, F. Melo, A. Sali, Comparative protein structure modeling of genes and genomes, Annu. Rev. Biophys. Biomol. Struct. 29 (2000) 291–325.
[43] S. Chakravarty, L. Wang, R. Sanchez, Accuracy of structure-derived properties in simple comparative models of protein structures, Nucleic Acids Res. 33 (2005) 244–259.
[44] N. Eswar, M.-A. Martí-Renom, B. Webb, M.S. Madhusudhan, D. Eramian, M. Shen, U. Pieper, A. Sali, Comparative protein structure modeling with Modeller, Curr. Protoc. Bioinforma. 15 (2006)(5.6.1.-5.6.30).
[45] S. Kelm, J. Shi, C.M. Deane, Medeller: homology-based coordinate generation for membrane proteins, Bioinformatics 26 (2010) 2833–2840.
[46] L.A. Kelley, M.J.E. Sternberg, Protein structure prediction on the web: a case study using the Phyre server, Nat. Protoc. 4 (2009) 363–371.
[47] S.H. White, W.C. Wimley, Membrane protein folding and stability; physical principles, Annu. Rev. Biophys. Biomol. Struct. 28 (1999) 319–365.
[48] K. Xie, T. Hessa, S. Seppälä, M. Rapp, G. von Heijne, R.E. Dalbey RE, Features of transmembrane segments that promote the lateral release from the translocase into the lipid phase, Biochemistry 46 (2007) 15153–15161.
[49] C. Snider, S. Jayasinghe, K. Hristova, S.H. White, MPeX: a tool for exploring membrane proteins, Protein Sci. 18 (2009) 2624–2628.
[50] F.X. Zhou, M.J. Cocco, W.P. Russ, A.T. Brunger, D.M. Engelman, Interhelical hydrogen bonding drives strong interactions in membrane proteins, Nat. Struct. Biol. 7 (2000) 154–160.
[51] F.X. Zhou, H.J. Merianos, A.T. Brunger, D.M. Engelman, Polar residues drive association of polyleucine transmembrane helices, Proc. Natl. Acad. Sci. U. S. A. 98 (2001) 2250–2255.
[52] H. Gratkowski, J.D. Lear, W.F. DeGrado, Polar side chains drive the association of model transmembrane peptides, Proc. Natl. Acad. Sci. U. S. A. 98 (2001) 880–885.
[53] M. Hermansson, G. von Heijne, Inter-helical hydrogen bond formation during membrane protein integration into the ER membrane, J. Mol. Biol. 334 (2003) 803–809.
[54] J.P. Dawson, J.S. Weineger, D.M. Engelman, Motifs of serine and threonine can drive association of membrane helices, J. Mol. Biol. 316 (2002) 799–805.
[55] E.L.R. Compton, N.A. Farmer, M. Lorch, J.M. Mason, K.M. Moreton, P.J. Booth, Kinetics of an individual transmembrane helix during bacteriorhodopsin folding, J. Mol. Biol. 357 (2006) 325–338.
[56] F.N. Barrera, D. Weerakkody, M. Anderson, O.A. Andreev, Y. Reshetnyak, D.E. Engelman, Roles of carboxyl groups in the transmembrane insertion of peptides, J. Mol. Biol. 413 (2011) 359–371.
[57] T. Hessa, S.H. White, G. von Heijne, Membrane insertion of a potassium-channel voltage sensor, Science 307 (2005) 1427.
[58] J.A. Freites, D.J. Tobias, G. von Heijne, S.H. White, Interface connections of a transmembrane voltage sensor, Proc. Natl. Acad. Sci. U. S. A. 102 (2005) 15059–15064.
[59] H.J. Butt, K. Fendler, E. Bamberg, J. Tittor, D. Oesterhelt, Aspartic acids 96 and 85 play a central role in the function of bacteriorhodopsin as a proton pump, EMBO J. 8 (1989) 1657–1663.
[60] H. Otto, T. Marti, M. Holtz, T. Mogi, L.J. Stern, F. Engel, H.G. Khorana, M.P. Heyn, Substitution of amino acids Asp-85, Asp-212, and Arg-82 in bacteriorhodopsin affects the proton release phase of the pump and the pK of the Schiff base, Proc. Natl. Acad. Sci. U. S. A. 87 (1990) 1018–1022.
[61] J.K. Lanyi, J. Tittor, G. Váró, G. Krippahl, D. Oesterhelt, Influence of the size and protonation state of acidic residue 85 on the absorption spectrum and photoreaction of the bacteriorhodopsin chromophore, Biochim. Biophys. Acta 1099 (1992) 102–110.
[62] D.A. Greenhalgh, S. Subramaniam, U. Alexiev, H. Otto, M.P. Heyn, H.G. Khorana, Effect of introducing different carboxylate-containing side chains at position 85 on chromophore formation and proton transport in bacteriorhodopsin, J. Biol. Chem. 267 (1992) 25734–25738.
[63] J. Heberle, D. Oesterhelt, N.A. Dencher, Decoupling of photo- and proton cycle in the Asp85 → Glu mutant of bacteriorhodopsin, EMBO J. 12 (1993) 3721–3727.
[64] A.-N. Bondar, J.C. Smith, S. Fischer, Structural and energetic determinants of primary proton transfer in bacteriorhodopsin, Photochem. Photobiol. Sci. 5 (2006) 547–552.
[65] A.-N. Bondar, C. del Val, J.A. Freites, D.J. Tobias, S.H. White, Dynamics of SecY translocons with translocation-defective mutations, Structure 18 (2010) 847–857.
[66] M. Nack, I. Radu, M. Gossing, C. Bamann, E. Bamberg, G.F. von Mollard, J. Heberle, The DC gate in channelrhodopsin-2: crucial hydrogen bonding interaction between C128 and D156, Photochem. Photobiol. Sci. 9 (2010) 194–198.
[67] G. Metz, F. Siebert, M. Engelhardt, Asp^{85} is the only internal aspartic acid that gets protonated in the M intermediate and the purple-to-blue transition of bacteriorhodopsin. A solid-state ^{13}C CP-Mas NMR investigation, FEBS Lett. 303 (1992) 237–241.
[68] R. Govindjee, M. Kono, S.P. Balashov, E. Imasheva, M. Sheves, T.G. Ebrey, Effects of substitution of tyrosine 57 with asparagine and phenylalanine on the properties of bacteriorhodopsin, Biochemistry 34 (1995) 4828–4838.
[69] P. Rath, M.P. Krebs, Y. He, H.G. Khorana, K.J. Rotschild, Fourier Transform Raman Spectroscopy of the bacteriorhodopsin mutant Tyr-185 ➔ Phe: formation of a stable O-like species during light adaptation and detection of its transient N-like photoproduct, Biochemistry 32 (1993) 2272–2281.
[70] C.P. Moon, K.G. Fleming, Side-chain hydrophobicity scale derived from transmembrane protein folding into lipid bilayers, Proc. Natl. Acad. Sci. U. S. A. 108 (2011) 10174–10177.
[71] M. Vijayakumar, H. Qian, H.-X. Zhou, Hydrogen bonds between short polar side chains and peptide backbone: prevalence in proteins and effects on helix-forming propensities, Proteins Struct. Funct. Genet. 34 (1999) 497–507.
[72] Y. Pilpel, N. Ben-Tal, D. Lancet, KPROT: a knowledge-based scale for the propensity of residue orientation in transmembrane segments, application to membrane protein structure prediction, J. Mol. Biol. 294 (1999) 921–935.
[73] C. del Val, S.H. White, A.-N. Bondar, Ser/Thr motifs in transmembrane proteins: conservation patterns and effects on local protein structure and dynamics, J. Membr. Biol. 245 (2012) 717–730.
[74] L. Adamian, J. Liang, Interhelical hydrogen bonds and spatial motifs in membrane proteins: polar clamps and serine zippers, Proteins Struct. Funct. Genet. 47 (2002) 209–218.
[75] T.M. Gray, B.W. Mathews, Intrahelical hydrogen bonds of serine, threonine and cysteine residues within a-helices and its relevance to membrane-bound proteins, J. Mol. Biol. 175 (1984) 75–81.
[76] L.G. Presta, G.D. Rose, Helix signals in proteins, Science 240 (1988) 1632–1641.
[77] J.S. Richardson, D.C. Richardson, Amino acid preferences for specific location at the ends of helices, Science 240 (1988) 1648–1652.
[78] A.J. Doig, W.M. Malcolm, B.J. Stapley, J.M. Thornton, Structures of N-termini of helices in proteins, Protein Sci. 6 (1997) 147–155.
[79] S. Kumar, M. Bansal, Dissecting a-helices: position-specific analysis of a-helices in globular proteins, Proteins Struct. Funct. Genet. 31 (1998) 460–476.
[80] M. Eilers, S.C. Shekar, T. Shieh, S.O. Smith, P.J. Fleming, Internal packing of helical membrane proteins, Proc. Natl. Acad. Sci. U. S. A. 97 (2000) 5796–5801.

[81] K. Welke, H.C. Watanabe, T. Wolter, M. Gaus, M. Elstner, QM/MM simulations of vibrational spectra of bacteriorhodopsin and channelrhodopsin-2, Phys. Chem. Chem. Phys. 15 (2013) 6651–6659.
[82] H.C. Watanabe, K. Welke, D.J. Sindhikara, P. Hegemann, M. Elstner, Towards an understanding of channelrhodopsin function: simulations lead to novel insights of the channel mechanism, J. Mol. Biol. 425 (2013) 1795–1814.
[83] B. Nie, J. Stutzman, A. Xie, A vibrational spectra marker for probing the hydrogen-bonding statis of protonated Asp and Glu residues, Biophys. J. 88 (2005) 2833–2847.
[84] T. Wada, K. Shimono, T. Kikukawa, M. Hato, N. Shinya, S.Y. Kim, T. Kimura-Someya, M. Shirozou, J. Tamogami, S. Miyauchi, K.-H. Jung, N. Kamo, S. Yokoyama, Crystal structure of the eukaryotic light-driven proton-pumping rhodopsin, *Acetabularia* rhodopsin II, from marine alga, J. Mol. Biol. 411 (2011) 986–998.
[85] M. Hatanaka, H. Kandori, A. Maeda, Localization and orientation of functional water molecules in bacteriorhodopsin as revealed by polarized Fourier transform infrared spectroscopy, Biophys. J. 72 (1997) 1001–1006.
[86] H. Luecke, B. Schobert, H.-T. Richter, J.-P. Cartailler, J.K. Lanyi, Structure of bacteriorhodopsin at 1.55 Å resolution, J. Mol. Biol. 291 (1999) 899–911.
[87] H. Luecke, Atomic resolution structures of bacteriorhodopsin photocycle intermediates: the role of discrete water molecules in the function of this light-driven proton pump, Biochim. Biophys. Acta 1460 (2000) 133–156.
[88] F. Garczareck, K. Gerwert, Functional waters in intraprotein proton transfer monitored by FTIR difference spectroscopy, Nature 439 (2005) 109–112.
[89] V.S. Bajaj, M.L. Mak-Jurkausas, M. Belenky, J. Herzfeld, R.G. Griffin, Functional and shunt states of bacteriorhodopsin revealed by 250 GHz dynamics nuclear polarization-enhanced solid-state NMR, Proc. Natl. Acad. Sci. U. S. A. 9 (2009) 9244–9249.
[90] H. Kandori, Hydration switch model for the proton transfer in the Schiff base region of bacteriorhodopsin, Biochim. Biophys. Acta 1658 (2000) 72–79.
[91] T. Kouyama, T. Nischikawa, T. Tokuhisa, H. Okumura, Crystal structure of the L intermediate of bacteriorhodopsin: evidence for vertical translocation of a water molecule during the proton pumping cycle, J. Mol. Biol. 335 (2004) 531–546.
[92] S. Hayashi, I. Ohmine, Proton transfer in bacteriorhodopsin: structure, excitation, IR spectra, and potential energy surface analyses by an ab initio QM/MM method, J. Phys. Chem. B 104 (2000) 10678–10691.
[93] K. Murata, Y. Fujii, N. Enomoto, M. Hata, T. Hoshino, M. Tsuda, A study on the mechanism of the proton transport in bacteriorhodopsin: the importance of the water molecule, Biophys. J. 79 (2000) 982–991.
[94] A.-N. Bondar, S. Fischer, J.C. Smith, M. Elstner, S. Suhai, Key role of electrostatic interactions in bacteriorhodopsin proton transfer, J. Am. Chem. Soc. 126 (2004) 14668–14677.
[95] A.-N. Bondar, M. Elstner, S. Suhai, J.C. Smith, S. Fischer, Mechanism of primary proton transfer in bacteriorhodopsin, Structure 12 (2004) 1281–1288.
[96] A.-N. Bondar, J. Baudry, S. Suhai, S. Fischer, J.C. Smith, Key role of active-site water molecules in bacteriorhodopsin proton transfer, J. Phys. Chem. B 112 (2008) 14729–14741.
[97] A.-N. Bondar, J.C. Smith, Water molecules in short- and long-distance proton transfer steps of bacteriorhodopsin proton pumping, Isr. J. Chem. 49 (2009) 155-161.
[98] A.-N. Bondar, S. Fischer, J.C. Smith, Water pathways in the bacteriorhodopsin proton pump, J. Membr. Biol. 239 (2011) 73–84.
[99] A.-N. Bondar, C. del Val, S.H. White, Rhomboid protease dynamics and lipid interactions, Structure 17 (2009) 395–405.
[100] A.-N. Bondar, S.H. White, Hydrogen bond dynamics in membrane protein function, Biochim. Biophys. Acta 1818 (2012) 942–950.
[101] M. Andersson, A.-N. Bondar, J.A. Freites, D.J. Tobias, H.R. Kaback, S.H. White, Proton-coupled dynamics in lactose permease, Structure 20 (2012) 1893–1904.
[102] T. Sattig, C. Rickert, E. Bamberg, H.-J. Steinhoff, C. Bamann, Light-induced movement of the transmembrane helix B in channelrhodopsin-2, Angew. Chem. Int. Ed. 52 (2013) 9705–9708.
[103] N. Krause, C. Engelhardt, J. Heberle, R. Schlesinger, R. Bittl, Structural differences between the closed and open states of channelrhodopsin-2 as observed by EPR spectroscopy, FEBS Lett. 587 (2013) 3309–3313.
[104] J. Kyte, R.F. Doolittle, A simple method for displaying the hydrophatic character of a protein, J. Mol. Biol. 157 (1982) 105–132.
[105] W. Humphrey, A. Dalke, K. Schulten, VMD: visual molecular dynamics, J. Mol. Graph. 14 (1996) 33–38.
[106] P. Emsley, K. Cowtan, *Coot*: model-building for molecular graphics, Acta Crystallogr. D60 (2004) 2126–2132.